FATIGUE STRENGTH OF NOTCHED CARBON STEEL SPECIMEN WITH A CIRCUMFERENTIAL CRACK AT THE NOTCH ROOT

URYU, Tsunemi
Research Institute for Applied Mechanics, Kyushu University

https://doi.org/10.5109/7162101

出版情報：Reports of Research Institute for Applied Mechanics. 5 (20), pp.129-141, 1957. 九州大学応用力学研究所

Reports of Research Institute for Applied Mechanics
Vol. V, No. 20, 1957

FATIGUE STRENGTH OF NOTCHED CARBON STEEL SPECIMEN WITH A CIRCUMFERENTIAL CRACK AT THE NOTCH ROOT*

By Tsunemi URYU

Abstract. Rotary bending tests were carried out with so-called compound-notched specimens, having deep hyperboloidal grooves of various root radii and circumferential cracks of various depths, and a calculation scheme for the fatigue strength of such compound-notched specimens was proposed. In this calculation the value of ε_C, the linear dimension of the fixed small plastic region at the tip of the crack, was considered to be about several hundredths of a millimeter for ordinary carbon steels.

1. Introduction. In the previous report,[1] concerning the fatigue strength of notched carbon steel specimens under reversed stresses, the *fatigue limit for crack initiation* of a notched specimen, which is the maximum nominal stress such that the specimen subjected to repetitions of this stress has no fatigue crack at the root of the notch, has been reasonably explained by considering the thickness of a surface layer, ε_0, concerned in the origin of fatigue crack. However, in the case of sharply notched specimens, the *usual fatigue limit*, i.e., the maximum nominal stress under which the specimen does not break off, is larger than the fatigue limit for crack initiation so that the specimen endured this usual fatigue limit has always a shallow circumferential non-propagating fatigue crack at the root of the notch. Therefore, the usual fatigue limit of the sharply notched specimen means the fatigue strength of the so-called compound-notched specimen with a shallow circumferential crack at the root of the machined notch (Such specimen will be called as the *compound-notched specimen* in the following).

In order to study such usual fatigue limits of sharply notched specimens as well as the fatigue strengths of compound-notched specimens with deeper cracks than non-propagating ones such as existed under the usual fatigue limits, rotary bending tests were carried out with compound-notched carbon steel specimens, having deep hyperboloidal grooves of various root radii and circumferential cracks of various depths, and a calculation scheme for the fatigue strength of such compound-notched specimens was proposed.

2. Materials and preparations of the compound-notched specimens. The materials used were two kinds of annealed carbon steels, 0.41 % C steel and

---

* Read before the 33rd General Meeting (Tokyo) of Japan Soc. Mech. Engs., April 2, 1956.

1) T. Isibasi, T.Uryu, "On the notch-factors of notched carbon steel specimens," Rep. Res. Inst. App. Mech., Kyushu Univ., IV, 1956, p. 107.

Table 1. Mechanical properties of the carbon steels used (Annealed state).

Steel	Annealing temp., °C	Yield point, kg/mm² Upper	Yield point, kg/mm² Lower	Tensile strength, kg/mm²	Actual breaking stress, σ_T, kg/mm²	Elongation (gauge, 50 mm) %	Contraction of area, %	Fatigue limit,* σ_{w0}, kg/mm²
0.41% C steel	830	39.3	37.6	62.7	105.4	30.4	50.4	28.5
0.23% C steel	860	30.9	28.3	47.9	81.6	34.1	54.0	21.75

* Fatigue limit under rotary bending of plain specimen.

0.23% C steel, which were the same materials as used in the previous study.[1] Their mechanical properties are reproduced in Table 1, and their microphotographs are shown in Fig. 8(a) and (b) at the end of the paper.

In order to make the compound-notched specimens, first, deep hyperboloidal-grooved specimens were made. The forms and dimensions of the deep hyperboloidal-grooved specimens were the same as those of the specimens used in the previous study[1] (Fig. 1).

Then, to make a circumferential fatigue crack at the root of the machined groove, these grooved specimens were subjected to uniform rotary bending stresses for proper numbers of stress repetitions according to wanted crack depths (Table 2). Although the depth of a developed crack depends roughly on the number of stress repetitions under the constant bending moment, to foresee more precisely the crack depth the machine was stopped many times in the course of stress repetitions and the deflection of the middle point of each specimen, due to statical bending moment, was measured with a Zeiss's dial indicator. And from the magnitude of such deflection the crack depth was estimated.

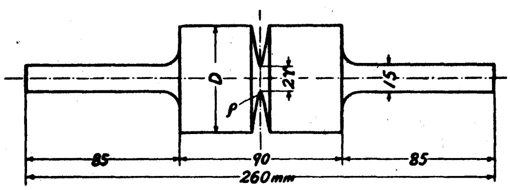

Steel	Outside dia., D, mm	Dia., $2r$, mm	Root radius, ρ, mm	Stress concent. factor
0.41% C steel	36	14	0.2	4.62
	"	"	0.5	3.04
	"	"	1.4	1.99
0.23% C steel	48	14	0.1	6.91
	"	"	0.2	4.62
	"	"	0.5	3.04
	"	"	1.4	1.99

Fig. 1. Forms and dimensions of deep hyperboloidal-grooved specimens.

Table 2. Cracking stress and number of stress repetitions for deep hyperboloidal-grooved specimens.

Steel	ρ, mm	Cracking stress,* kg/mm²	No. of repetitions, × 10⁴
0.41% C steel	0.2	14.5	31~32
	0.5	15.5	25~45
	1.4	20.0	19~40
0.23% C steel	0.1	16.0	17~34
	0.2	"	19~26
	0.5	"	13~26
	1.4	16.0~17.5	19~40

* Nominal stress based on the notched section.

After the crack of wanted depth was developed, such cracked specimens were packed together with steel cutting chip in a tight steel box, to prevent excessive oxidation of their surfaces, and they were annealed at 650°C for 30 min., in order to relieve the strain-hardening around the tip of the crack due to cracking. Thus the compound-notched specimens were completed.

3. Results of the experiments. The results obtained by rotary bending tests on the compound-notched specimens are summarized in Table 3

Table 3. Results of rotary bending tests on compound-notched specimens with circumferential cracks at the roots of deep hyperboloidal grooves (0.41% C steel).

ρ, mm	Specimen No.	$2r$, mm	$2a$, mm	$2b$, mm	λ_c, mm	e, mm	Applied bending moment, M, kg-m	No. of repetitions,* $\times 10^6$	ρ_c, mm	Fatigue strength, M_e, kg-m
0.2	21	13.99	12.27	12.23	1.075	0.159	2.42 2.92	10.1 (NB) 3.4 (B)	0.047	2.51
	23	13.99	11.77	11.09	1.618	0.167	2.56	1.5 (B)	0.046	2.30
0.5	12	13.99	13.40	13.31	0.337	0.002	2.76 3.60	13.8 (NB) 0.5 (B)	0.133	2.71
	13	14.00	13.63	12.73	0.649	0.017	2.96	1.2 (B)	0.092	2.73
	14	14.02	13.45	12.81	0.665	0.061	2.44 3.25	10.5 (NB) 0.8 (B)	0.090	2.70
	11	14.01	13.71	12.75	0.669	0.040	2.70 3.51	9.0 (NB) 0.7 (B)	0.090	2.74
	17	14.00	13.42	12.45	0.915	0.138	2.55	4.0 (B)	0.075	2.60
	19	13.98	12.88	12.24	0.925	0.055	2.68	1.2 (B)	0.075	2.57
	18	13.98	11.94	12.36	1.213	0.381	2.43 3.23	10.7 (NB) 0.7 (B)	0.065	2.36
	10	14.03	12.88	11.59	1.312	0.094	2.97	0.8 (B)	0.063	2.53
1.4	31	13.96	13.39	13.11	0.707	0.282	3.08 3.74	10.0 (NB) 0.8 (B)	0.372	3.26
	33	13.94	13.94	13.04	0.904	0.452	2.66 3.45	4.3 (NB) 2.1 (B)	0.317	3.18
	41	13.97	13.11	12.16	1.021	0.116	3.49	0.9 (B)	0.290	3.02
	36	14.00	14.00	11.51	1.370	0.128	3.23	1.4 (B)	0.232	3.01
	42	13.92	13.69	11.41	1.423	0.188	3.10	0.6 (B)	0.225	2.98
	37	13.99	13.61	11.43	1.455	0.174	2.96	1.5 (B)	0.221	2.93
	40	13.99	13.99	11.57	1.458	0.247	3.63	0.7 (B)	0.221	2.94
	34	13.97	13.97	11.61	1.618	0.437	2.81 3.62	11.0 (NB) 1.5 (B)	0.203	2.88
	38	13.99	12.97	11.07	1.845	0.422	2.82 3.76	14.2 (NB) 1.0 (B)	0.181	2.61
	39	13.98	12.34	10.91	1.856	0.319	2.88	1.3 (B)	0.180	2.53

* (NB) indicates that specimen did not break; (B) indicates that specimen broke off.

for 0.41 % C steel and in Table 4 for 0.23 % C steel. (The speed of stress repetitions was about 2500 ~ 2700 rpm.). In these tables, $2a$ and $2b$ in the 4th and 5th columns, respectively, are the dimensions of the actual residual part at the cracked section and λ_c in the 6th column is the depth of original

Table 4. Results of rotary bending tests on compound-notched specimens with circumferential cracks at the roots of deep hyperboloidal grooves (0.23 % C steel).

ρ, mm	Specimen No.	$2r$, mm	$2a$, mm	$2b$, mm	λ_c, mm	e, mm	Applied bending moment, M, kg-m	No. of repetitions,* $\times 10^6$	ρ_c, mm	Fatigue strength, M_e, kg-m
0.1	0-11	14.00	12.70	12.59	0.755	0.053	2.63 3.30	11.5 (NB) 1.0 (B)	0.085	2.61
	1-16	14.01	12.40	12.19	1.104	0.211	2.50	2.6 (B)	"	2.55
	1-17	13.99	11.42	11.30	1.421	0.028	2.40	1.3 (B)	"	2.39
	1-22	13.99	11.81	11.56	1.471	0.260	2.20 2.60	9.9 (NB) 0.6 (B)	"	2.40
0.2	0-7	13.93	12.38	12.00	1.235	0.269	2.50	3.6 (B)	0.086	2.49
	1-13	13.97	12.09	11.83	1.266	0.197	2.35 2.95	6.8 (NB) 1.4 (B)	"	2.48
	1-12	14.00	12.12	11.89	1.348	0.301	2.70	0.9 (B)	0.085	2.46
	1-15	14.00	11.83	11.12	1.626	0.190	2.10 2.60	7.2 (NB) 1.1 (B)	"	2.39
	0-6	13.85	10.73	10.41	1.831	0.111	2.20	2.7 (B)	"	2.07
0.5	2-4	14.01	13.09	12.85	0.671	0.092	2.50 3.50	8.0 (NB) 0.8 (B)	0.126	2.63
	2-2	13.97	12.42	12.36	0.864	0.058	2.70 3.30	11.7 (NB) 1.4 (B)	0.115	2.56
	2-6	13.98	12.20	12.19	0.899	0.033	2.40	2.1 (B)	0.113	2.48
	2-5	13.99	12.54	12.37	0.954	0.144	2.70	1.1 (B)	0.111	2.54
	2-3	14.01	11.94	12.05	1.121	0.142	2.15 2.80	9.2 (NB) 1.1 (B)	0.106	2.41
1.4	2-11	13.97	—	—	0.228**	—	2.90 3.50	10.1 (NB) 1.2 (B)	0.672	3.17
	2-7	13.98	13.16	13.40	0.414	0.120	2.60 3.20	10.1 (NB) 0.7 (B)	0.528	2.98
	2-10	13.99	13.62	13.04	0.492	0.020	2.80 3.40	8.4 (NB) 0.9 (B)	0.486	2.98
	2-8	13.98	13.48	12.71	0.681	0.045	2.85	1.4 (B)	0.411	2.91
	2-9	13.97	13.48	12.74	0.692	0.080	2.90	3.1 (B)	0.411	2.90
	1-20	13.98	13.16	12.78	0.729	0.132	2.70 3.50	10.2 (NB) 0.6 (B)	0.395	2.85
	1-19	14.00	13.46	12.46	1.188	0.415	2.70	1.4 (B)	0.294	2.76
	1-2	13.98	12.28	11.66	1.846	0.690	2.20	2.4 (B)	0.217	2.39

* (NB) indicates that specimen did not break; (B) indicates that specimen broke off.
** Crack was only in a part of circumference.

crack (referring to Fig. 2). Their magnitudes were able to be measured with a micrometer-microscope, after each specimen was broken since the original cracked region A (Fig. 2) was coloured due to annealing after cracking. As seen in Fig. 2, the original crack depth of each specimen was not uniform along the circumference of the section. In such case, the distance *QP* was regarded as the original crack depth λ_c of the specimen since the crack advanced the battered region B (Fig. 2) due to stress repetitions was observed to start from the point *P* and its vicinity by inspecting the appearances of the fractured surfaces. Therefore, in such cases that the specimens did not break under certain bending moments, they were subjected to higher bending moments than before in order to break off them without any noticeable deformation. Some fractured surfaces of the compound notched specimens are shown in Fig. 10 at the end of the paper.

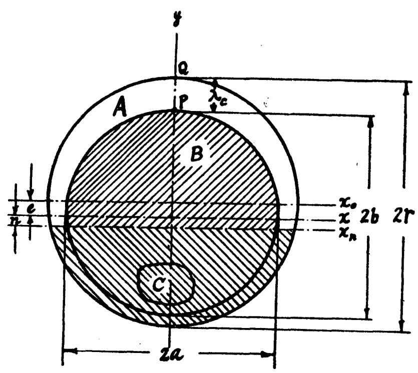

A; Original cracked region.
B; Battered region.
C; Final fractured region.

Fig. 2. Fractured surface of compound-notched specimen (Schematic).

4. Calculation scheme for the fatigue strength of compound-notched specimens. Now, in order to discuss the above experimental results, the fatigue strength under rotary bending of a compound notched bar with a circumferential crack of *uniform depth* will be calculated under the following considerations.

(1) In order to make the original crack develop further in fatigue, it will be necessary that the fixed small region at the tip of the crack is subjected to such repeated stress that this small region is plastically deformed repeatedly,[2),3)] and a new fatigue crack will be made in such small plastic region after a certain number of stress repetitions.

Here, we assume that the magnitude of this fixed small plastic region is represented by the linear dimension, ε_c, measured from the tip of the original crack in the direction of the propagation of the fatigue crack (Fig. 3) and the magnitude of such ε_c depends

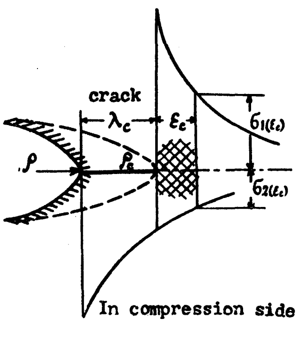

Fig. 3.
Stress distributions around the tip of crack at the root of machined notch in bending.

---

2) T. Isibasi, "The mechanism of fatigue crack propagation in carbon steels and the fatigue limits of notched bars," Proc. 8th Interntl. Congress Theor. App. Mech., 1953, p. 216.

3) A. K. Head, "The growth of fatigue cracks," Phil. Mag., 44, 1953, p. 925.

on the material but not on the depth of the original crack.

(2) It is, now, difficult to know the exact stress distribution around the tip of the crack in the compound-notched bar subjected to bending moment, so we estimate simply such stress distribution around the tip of the crack as follows.

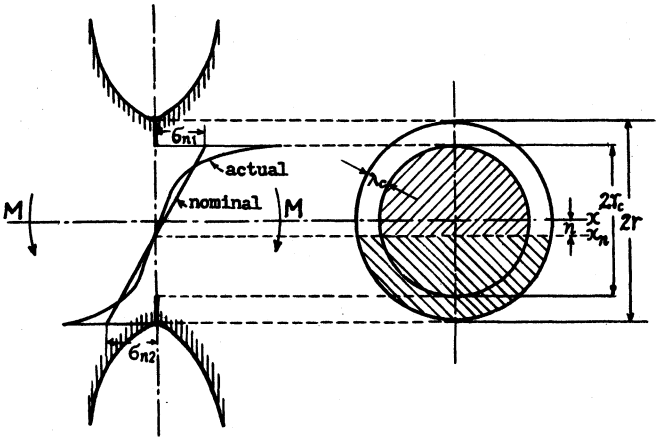

(a) Stress distribution. (b) Cracked section.

Fig. 4. Cracked section in compound-notched bar with a circumferential crack of uniform depth.

First, the moment of inertia I of the cracked section is calculated by assuming that the cracked part supports the compressive stress but not the tensile one while the stress distribution is linear as in ordinary bending.[4] Namely, I is the moment of inertia of the shaded area about x_n-axis (the neutral axis, of which the position is n) as shown in Fig. 4 (b). Therefore, the nominal tensile stress σ_{n1} and the nominal compressive one σ_{n2} (Fig. 4 (a)) are presented as follows;

$$\left.\begin{aligned} \sigma_{n1} &= \frac{M}{I}(r_c + n) \\ \sigma_{n2} &= \frac{M}{I}(r - n) \end{aligned}\right\}, \tag{1}$$

where, M is the bending moment, r_c is the radius of the actual residual section, and n and I can be calculated by using the formulae in the paper.[4]

Then, concerning the stress concentration factors around the tip of the crack in the tension side, we suppose that the crack, including the outer machined groove, is equivalent to a deep hyperboloidal groove of the root radius

$$\rho_c = (\rho - \varepsilon_c) \exp\left(-2\sqrt{\frac{\lambda_c}{\rho}}\right) + \varepsilon_c. \tag{2}$$

This empirical formula (2) for the equivalent root radius ρ_c of the tip of the crack will be used so far as $\rho \geqq \varepsilon_c$ but not so large. In the compression side, on the other hand, we suppose that the crack has no stress concentration effect; that is, the stress distribution around the tip of the crack is

[4] R. E. Peterson, "Stress-concentration phenomena in fatigue of metals," Trans. ASME, 55, 1933, p. 157.

given only by the stress concentration effect of the machined groove (Figs. 3 and 4). Consequently, in both tension and compression sides, we can calculate the stress concentration factors around the tip of the crack by means of Neuber's method for the deep hyperbolidal groove.[5]

Here, to confirm the above assumptions, a photoelastic model (Epoxy resin) of the plate specimen with semicircular notches on both sides, containing a crack at the root of the notch only on one side, was examined under uniform bending moments (Fig. 9 (a) and (b) at the end of the paper). In Fig. 9 (a), in which the cracked part is in the tension side, the high stress concentration at the tip of the crack is seen. In Fig. 9 (b), on the other hand, in which the cracked part is in the compression side, the stress distribution around the tip of the crack is actually the same as the distribution due to the machined notch.

(3) The total stresses in the fixed small plastic region, ε_c, at the tip of the original crack is considered to have predominant effect on the initiation of a new fatigue crack in that region. Thus, we may consider that a new fatigue crack is initiated in such plastic region when the actual stress at the point distant ε_c from the tip of the original crack exceeds the fatigue limit of the plain specimen. In the present case, the repeated stress at such point varies from the tensile stress $\sigma_{1(\varepsilon_c)}$ to the compressive one $\sigma_{2(\varepsilon_c)}$ (Fig. 3); that is,

$$\left.\begin{array}{ll}\text{the stress amplitude,} & \sigma_{r(\varepsilon_c)} \\ \text{the mean stress,} & \sigma_{m(\varepsilon_c)}\end{array}\right\} = \frac{1}{2}\left[\sigma_{1(\varepsilon_c)} \pm \sigma_{2(\varepsilon_c)}\right] = \frac{M}{2I}\left[(r_c + n)\,\alpha_{1(\varepsilon_c)} \pm (r - n)\,\alpha_{2(\varepsilon_c)}\right], \qquad (3)$$

in which, $\alpha_{1(\varepsilon_c)}$ and $\alpha_{2(\varepsilon_c)}$ are the stress concentration factors at the point distant ε_c from the tip of the crack in the tension and compression sides, respectively, calculated by means of Neuber's method.[5]

Therefore, the fatigue strength under rotary bending of the compound-notched bar can be determined with the following formulae;

$$\left.\begin{array}{l}\sigma_{r(\varepsilon_c)} = \sigma_{r0} \\ \sigma_{m(\varepsilon_c)} = \sigma_{m0}\end{array}\right\}. \qquad (4)$$

Where, σ_{r0} and σ_{m0} are the stress amplitude and the mean stress of the fatigue limit of the plain specimen, respectively, such as given in the fatigue limit diagram (Fig. 5). From the formulae (4), in the result, we can obtain the fatigue strength of the compound-notched bar, M_c, in the form of bending moment, i.e.,

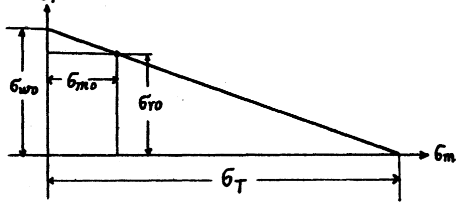

Fig. 5. Fatigue limit diagram for the plain specimen (σ_{w0} and σ_T are presented in Table 1).

[5] H. Neuber, "Kerbspannungslehre," Julius Springer, Berlin, 1937.

$$M_c = \frac{2I\sigma_{w0}}{[(r_c+n)\alpha_{1(\varepsilon_c)}+(r-n)\alpha_{2(\varepsilon_c)}]+[(r_c+n)\alpha_{1(\varepsilon_c)}-(r-n)\alpha_{2(\varepsilon_c)}]\frac{\sigma_{w0}}{\sigma_T}}. \quad (5)$$

In the case of the compound-notched specimens used in the present experiments, the original crack depth is not uniform along the circumference as shown schematically in Fig. 2. In such case, the fatigue strength of each specimen will be determined depending on the stress at the point P (Fig. 2). Regarding the region B in Fig. 2 as an elliptical form with the axes $2a$ and $2b$ (the position of the centre is e), the position of the neutral axis, n, can be found in the following formula by using the trial and error method;

$$\frac{a}{b}\left[\frac{2}{3}\sqrt{(b^2-n^2)^3}+n^2\sqrt{b^2-n^2}+b^2n\left(\sin^{-1}\frac{n}{b}+\frac{\pi}{2}\right)\right]$$
$$-\left[\frac{2}{3}\sqrt{\{r^2-(n\pm e)^2\}^3}+(n\pm e)^2\sqrt{r^2-(n\pm e)^2}\right.$$
$$\left.+r^2(n\pm e)\left(\sin^{-1}\frac{n\pm e}{r}-\frac{\pi}{2}\right)\right]=0. \quad (6)$$

And the moment of inertia I of the cracked section becomes as follows;

$$I=\frac{2a}{b}\left[\frac{5}{12}n\sqrt{(b^2-n^2)^3}+\left(\frac{b^2}{8}+\frac{n^2}{2}\right)\left\{n\sqrt{b^2-n^2}+b^2\left(\sin^{-1}\frac{n}{b}+\frac{\pi}{2}\right)\right\}\right]$$
$$-\left[\frac{5}{6}(n\pm e)\sqrt{\{r^2-(n\pm e)^2\}^3}\right.$$
$$\left.+\left\{\frac{r^2}{4}+(n\pm e)^2\right\}\left\{(n\pm e)\sqrt{r^2-(n\pm e)^2}+r^2\left(\sin^{-1}\frac{n\pm e}{r}-\frac{\pi}{2}\right)\right\}\right]. \quad (7)$$

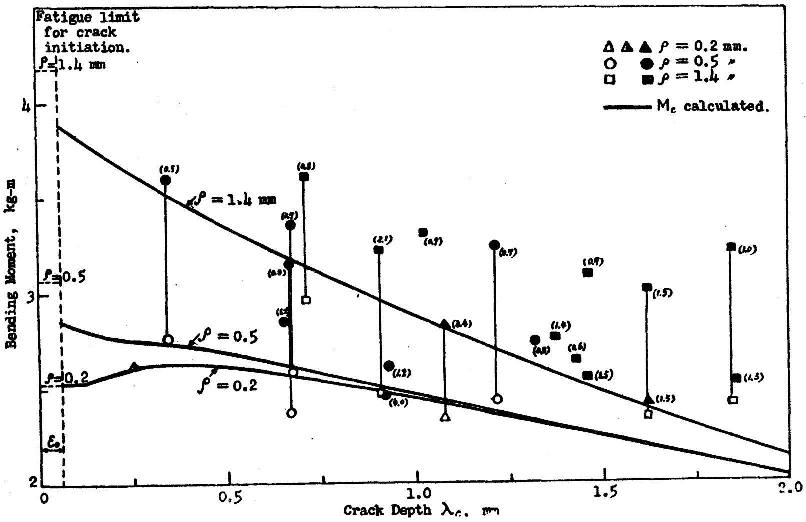

Fig. 6. Fatigue strength M_c under rotary bending of compound-notched bars with circumferential crack of uniform depth λ_c (0.41% C steel, $\varepsilon_c = 0.045$ mm, $2r = 14$ mm).

For the formulae (6) and (7), we denote, $n=n_1$ and $I=I_1$ in case of $+e$ (the point P in tension side), and $n=n_2$ and $I=I_2$ in case of $-e$ (the point P in compression side). Therefore, in this case, the fatigue strength of the compound-notched specimen, M_e, can be expressed as follows;

$$M_e = \frac{2\sigma_{w0}}{\left[\frac{(b+n_1)\alpha_{1(\varepsilon_C)}}{I_1} + \frac{(r-n_2+e)\alpha_{2(\varepsilon_C)}}{I_2}\right] + \left[\frac{(b+n_1)\alpha_{1(\varepsilon_C)}}{I_1} - \frac{(r-n_2+e)\alpha_{2(\varepsilon_C)}}{I_2}\right]\frac{\sigma_{w0}}{\sigma_T}} . \qquad (8)$$

5. Numerical calculations. The fatigue strengths M_c of compound-notched bars, varying ρ and λ_c when $2r=14$ mm constant, were numerically calculated by the formula (5), assuming the suitable values of ε_c to be 0.045 mm for 0.41 % C steel and 0.085 mm for 0.23 % C steel. The results obtained are shown with the solid curves in Figs. 6 and 7 for 0.41 % C steel and 0.23 % C steel, respectively. In these figures, for reference, the fatigue limits for crack initiation as well as the usual fatigue limits of deep hyperboloidal-grooved specimens without the original cracks, obtained in the previous study[1], are shown with the vales of bending moment.

Then, to prove the above calculation scheme in comparison with the experimental results, the fatigue strength M_e of each specimen in Tables 2 and 3 was computed by the formula (8), as shown in the last columns in those tables. It is seen that M_e explain considerably well the experimental

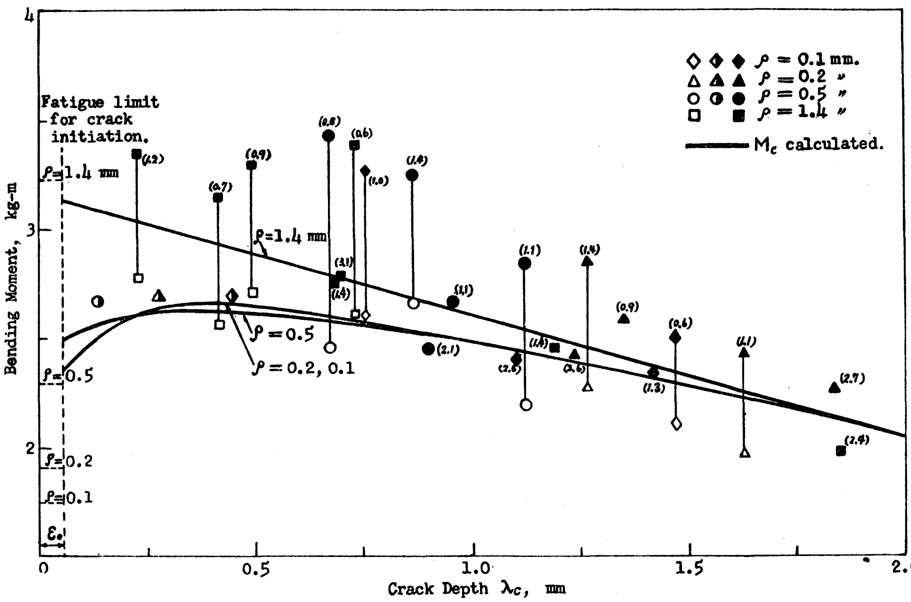

Fig. 7. Fatigue strength M_c under rotary bending of compound-notched bars with circumferential crack of uniform depth λ_c (0.23 % C steel, $\varepsilon_c=$ 0.085 mm, $2r=14$ mm).

results, i.e., the applied bending moments M and the according numbers of stress repetitions to failure.

Moreover, to show graphically, the values of $M(M_c/M_e)$ instead of M for each specimen are plotted against its crack depth λ_c in Figs. 6 and 7. In these figures, the open points show that the specimens did not break and the solid points show that the specimens broke (Nos. in parentheses are the numbers of stress repetitions to failure in 10^6 cycles), and it means one specimen to connect the open point and the solid one by a straight line, and the half solid points show the above-mentioned usual fatigue limits of deep hyperboloidal-grooved specimens against their non-propagating crack depths.

Although, in the above numerical calculations, we had to assume a suitable value of ε_c for the material, the value of ε_c will be about several hundredths of a millimeter for a ordinary carbon steel, and its magnitude may be considered to express the crack sensitivity of the material in fatigue.

According to the above considerations about the fatigue strength of compound-notched specimens, it will be expected that two kinds of the fatigue limits of sharply notched specimens are discriminated in the case of reversed stresses (such as, rotary bending,[1),6)] reversed tension and compression[7),8)]), but not in the case of pulsating stresses. In the latter case the specimens are necessarily broken off if a crack is initiated at the root of the notch and the operating load remains unchanged.

6. Conclusions. Following conclusions will be obtained from the above results.

(1) The fatigue strengths under rotary bending of compound notched carbon steel specimens, having deep hyperboloidal grooves of various root radii and circumferential cracks of various depths, were obtained (Tables 2 and 3).

(2) A calculation scheme for the fatigue strength of such compound-notched specimens was proposed.

(3) In the above calculation the value of ε_c, the linear dimension of the fixed small plastic region at the tip of the crack, may be considered to be about several hundredths of a millimeter for ordinary carbon steels.

Acknowledgements: The author wishes to express his hearty thanks to Professor T. Isibasi of Kyushu University for his guidance and encouragement during this study. And he thanks to the assistance of Mr. M. Kobayashi of this Institute in the experimental work.

(Received July 30, 1957)

6) J. M. Lessells, H. E. Jacques, "Effect of fatigue on transition temperature of steel," The Welding Jour., 29, 1950, Res. Suppl., p. 74-s.

7) A. J. Fenner, N. B. Owen, C. E. Phillips, "The fatigue crack as a stress-raiser," Engineering, 171, 1951, p. 637.

8) N. E. Frost, "Crack formation and stress concentration effects in direct stress fatigue," Engineer, 200, 1955, p. 464 and p. 501.

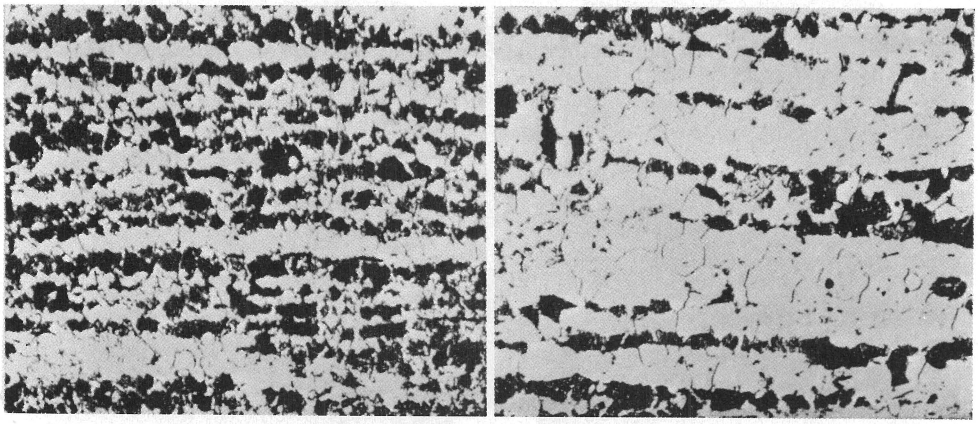

(a) 0.41 % C steel. (b) 0.23 % C steel.

Fig. 8. Microphotographs of the steels used (× 150).

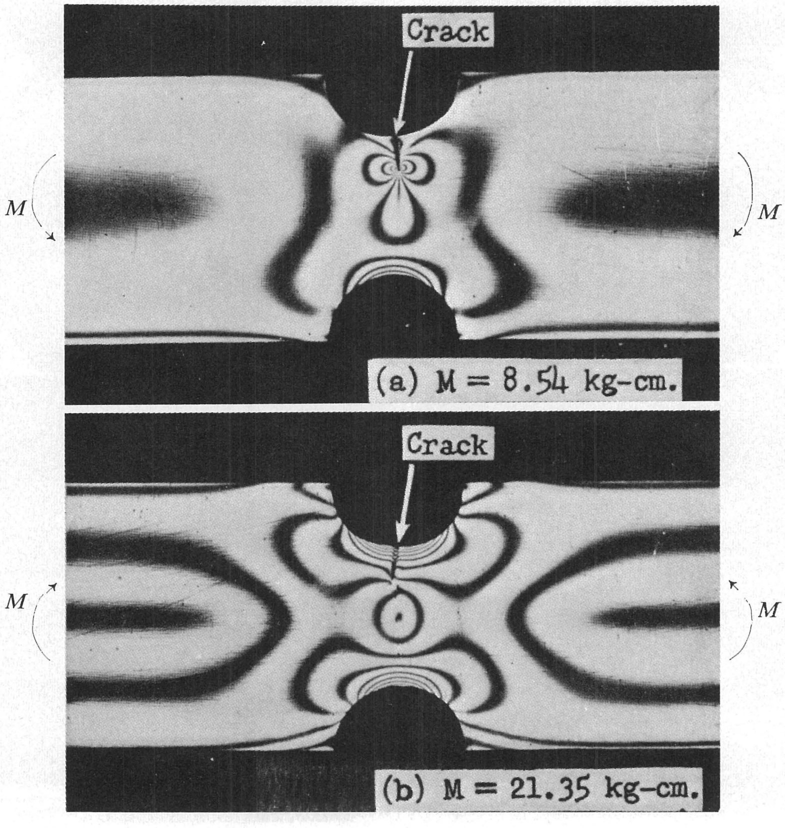

Fig. 9. Isochromatic-fringe photographs of a semicircular-notched plate specimen with a crack in uniform bending.

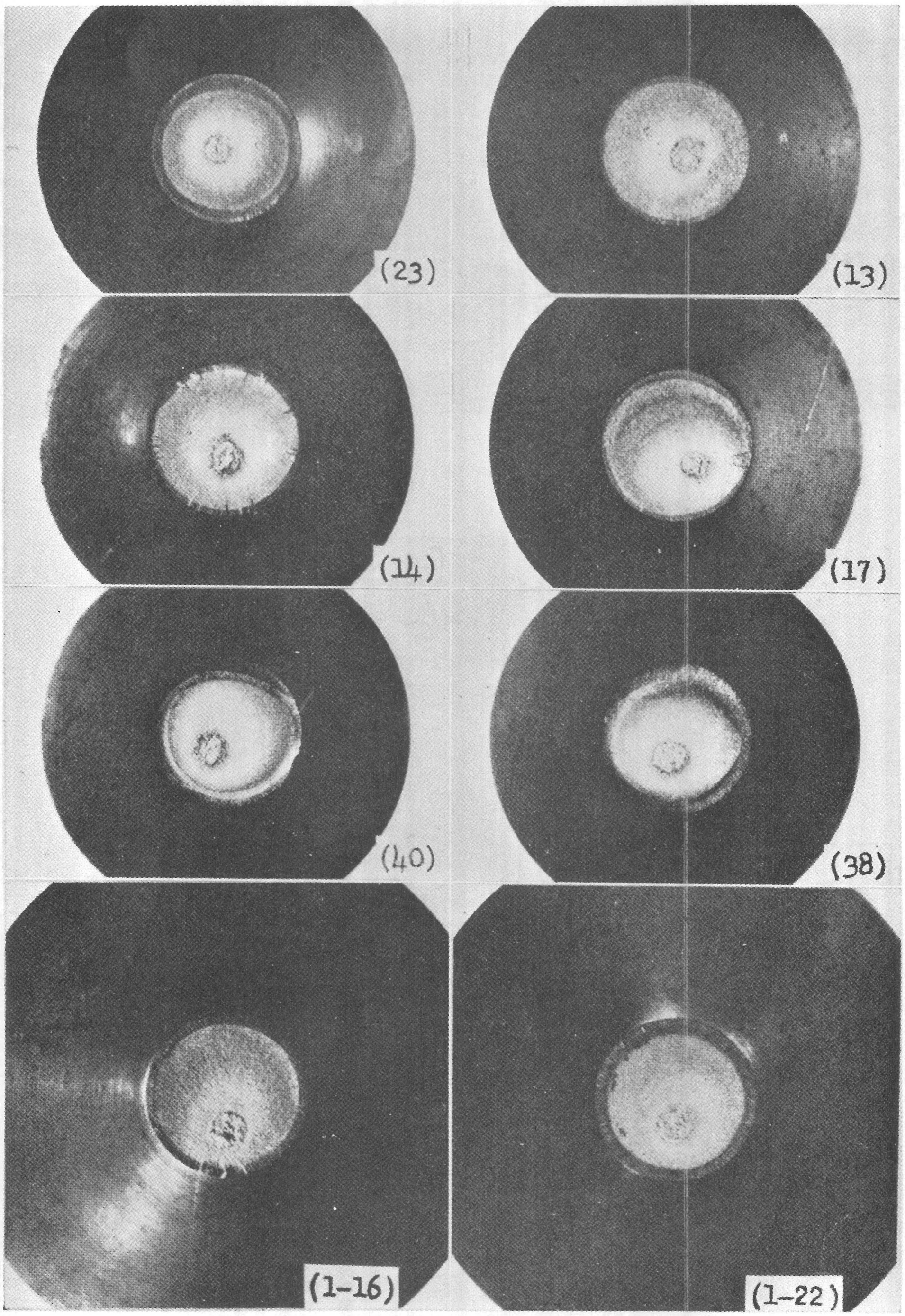

Fig. 10. Fractured surfaces of compound-notched specimens
(Nos. in parentheses are specimen Nos. $\times$ 1.5).

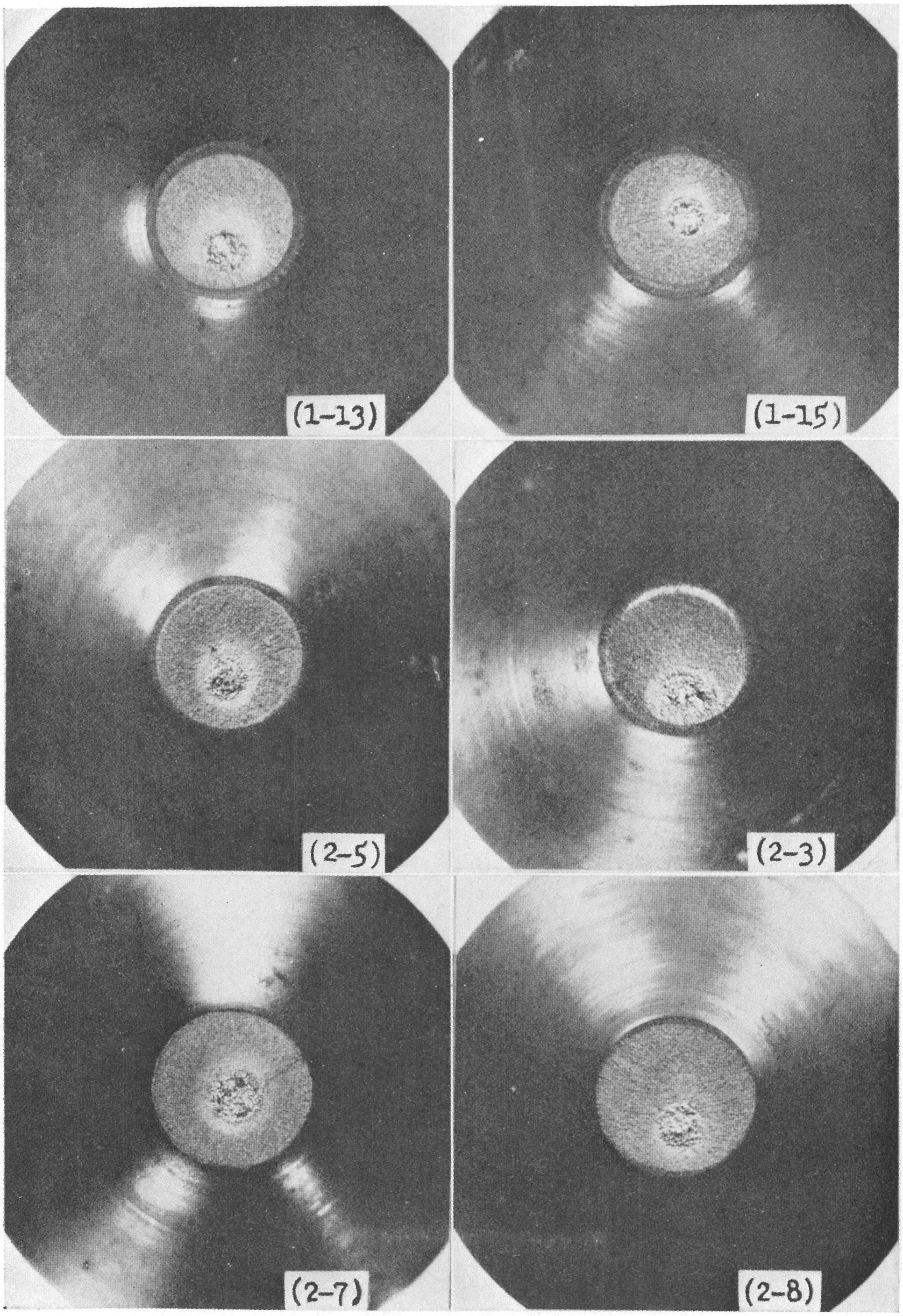

Fig. 10. (Continued).